Ablation of *Ctrp9*, Ligand of AdipoR1, and Lower Number of Cone Photoreceptors in Mouse Retina

Daiki Inooka,[1] Yoshihiro Omori,[2] Noriyuki Ouchi,[3] Koji Ohashi,[3] Yuto Kawakami,[2] Yoshito Koyanagi,[1,4] Chieko Koike,[5] Hiroko Terasaki,[1] Koji M. Nishiguchi,[1] and Shinji Ueno[1]

[1]Department of Ophthalmology, Nagoya University Graduate School of Medicine, Nagoya, Japan
[2]Laboratory of Functional Genomics, Graduate School of Bioscience, Nagahama Institute of Bioscience and Technology, Shiga, Japan
[3]Department of Molecular Medicine and Cardiology, Nagoya University Graduate School of Medicine, Nagoya, Japan
[4]Department of Ophthalmology, Graduate School of Medical Sciences, Kyushu University, Fukuoka, Japan
[5]College of Pharmaceutical Sciences, Ritsumeikan University, Kusatsu, Shiga, Japan

Correspondence: Shinji Ueno, Department of Ophthalmology, Nagoya University Graduate School of Medicine, 65 Tsuruma-cho, Showa-ku, Nagoya 466-8550, Japan; ueno@med.nagoya-u.ac.jp.

Received: August 19, 2021
Accepted: April 26, 2022
Published: May 16, 2022

Citation: Inooka D, Omori Y, Ouchi N, et al. Ablation of *Ctrp9*, ligand of AdipoR1, and lower number of cone photoreceptors in mouse retina. *Invest Ophthalmol Vis Sci.* 2022;63(5):14. https://doi.org/10.1167/iovs.63.5.14

Purpose. C1q/TNF-related protein (CTRP) 9 is one of the adiponectin paralogs, and a genetic ablation of its receptor, AdipoR1, is known to cause retinal degeneration. The purpose of this study was to determine the role played by CTRP9 in the retina.

Methods. The retinas of *Ctrp9* gene knockout (KO) and wild type (WT) mice were examined by electroretinography (ERG), histology, RNA sequencing, and quantitative real-time PCR.

Results. The amplitude of the photopic ERG elicited by the maximum stimulus intensity was smaller by 40% in the *Ctrp9* KO mice than in WT mice at 8 weeks of age. However, the photopic ERGs was not reduced from 8 weeks to 6 months of age. The amplitudes of the scotopic ERGs were not reduced in the *Ctrp9* KO mice at 8 weeks and 6 months of age. No distinct histological abnormalities were found in the retinal sections but the density of peanut agglutinin-stained cells in the retinal flat mount of KO mice was reduced to about 70% of that of WT mice. Genomewide RNA sequencing of the retina revealed the absence of the expression of CTRP9 in both KO and WT mice. RNA sequencing and quantitative real-time PCR analysis showed that the expressions of the transcripts of genes expressed in cones, *Opn1sw*, *Opn1mw*, *Gnat2*, and *Cnga3*, were reduced in the KO mice retina, however, the degree of expression of the transcripts in rods was not significantly reduced.

Conclusions. CTRP9 is released ectopically from other tissues, and it regulates the number of cones in the mouse retinas.

Keywords: C1q/TNF-related protein 9 (CTRP), adiponectin, electroretinography (ERG), RNA sequencing, reduction of cone number

The C1q/TNF-related proteins (CTRPs) contain a collagen-like domain, the C1q-like domain, which is classified as an adiponectin paralog because of its structural similarities to adiponectin.[1,2] In recent years, the CTRP family of proteins has attracted much interest by scientists because of their anti-inflammatory and insulin-sensitizing effects. CTRP9 is one of the adiponectin paralog belonging to the CTRP family, and it is expressed predominantly in adipose tissues, skeletal muscles, mammary glands, and heart.[3] It plays beneficial roles in the regulation of inflammation, oxidative stress, glucose metabolism, and vascular function as an adipocytokine through the adiponectin receptor1, ADIPOR1.[4–6]

ADIPOR1 was initially described as an adiponectin receptor that regulated the metabolism of systemic lipid and glucose.[7] It has recently been reported that ADIPOR1 also plays critical roles in the retina.[8–10]

AdipoR1 deficient mice develop retinal degeneration due to an impaired uptake of docosahexaenoic acid (DHA).[11] In humans, mutations of ADIPOR1 cause retinitis pigmentosa with or without systemic disorders.[8,9] Immunohistochemical studies have confirmed that the ADIPOR1 protein is present in the retina with the strongest signals appearing in the photoreceptor outer segments and weaker signals appearing in the rest of the neural retina, including the outer nuclear layer and the retinal pigment epithelium.[10] The importance of ADIPOR1 in the retina has been documented in several studies, however, the influence of signaling-related ADIPOR1 has not been determined. Mice deficient of adiponectin, another ligand of ADIPOR1, did not show any retinal abnormalities,[11] and it was suggested that ADIPOR1 can act independently of adiponectin in the maintenance of the photoreceptors. Only a few studies have examined the role played by CTRP9 in retinal tissues. In vitro analysis

showed that CTRP9 can prevent apoptosis in human retinal pigment epithelial (ARPE-19) cells exposed to high glucose levels.[12] Nevertheless, the role of CTRP9 in the retina has not been definitively determined.

Thus, the purpose of this study was to determine the role played by CTRP9 in the physiology and morphology of the retina. To accomplish this, we examined the physiological and morphological characteristics of the retina of *Ctrp9* gene knockout (KO) mice. The findings in the *Ctrp9* KO mice were compared to those in wild type (WT) mice.

Materials and Methods

Animals

WT and *Ctrp9* KO mice on a C57/BL6J background were studied.[6] The *Ctrp9* KO mice were created from an embryonic stem cell clone (C1qtnf9_AE11), generated by Regeneron Pharmaceuticals, Inc. (Tarrytown, NY, USA), the KOMP Repository (www.komp.org), and the Mouse Biology Program (www.mousebiology.org) at the University of California Davis.[13] The genotyping primers for the *Ctrp9* WT allele were:

5′-CCTGCACACCAAGGACAGTTAC-3′ (forward) and
5′-TGTCACCTGCATCCACACTTC-3′ (reverse).

Primers for the *Ctrp9*-null allele were:

5′-GGTAAACTGGCTCGGATTAGGG-3′ (forward) and
5′-TTGACTGTAGCGGCTGATGTTG-3′ (reverse).

Homozygous *Ctrp9* KO and WT littermates were used in this study. All experimental procedures adhered to the ARVO statement for the use of animals in ophthalmic and vision research and the guidelines for the use of animals of the Nagoya University School of Medicine. The Nagoya University animal experiment committee approved this project (Approval Number, 20106).

Electroretinography Recordings

The procedures used to record the electroretinographies (ERGs) were similar to those described in detail.[14] The mice were dark-adapted for at least 2 hours before the ERG recordings. The mice were placed in a Ganzfeld bowl (Model GS2000; LACE Electronica sel via Marmiccilo, Pisa, Italy). Six stimulus intensity steps ranging from −5.0 to 1.0 log cd s/m^2 were used to elicit the scotopic ERGs, and 4 stimulus intensity steps ranging from −0.8 to 1.0 log cd s/m^2 were used to elicit the photopic ERGs. The photopic ERGs were recorded 10 minutes after turning on the adapting background light of 40 cd/m^2. The ERGs were averaged using a computer-assisted signal averaging system (Power Lab; AD Instruments, Castle Hill, Australia). Seven WT mice and 10 KO mice were evaluated at 8 weeks of age, and 6 WT mice and 8 KO mice were evaluated at 24 weeks of age.

Retinal Histology

The retinas of 3 WT mice and 3 KO mice at 8 weeks and 24 weeks were studied histologically by hematoxylin and eosin (H&E) staining. Eyes were embedded in paraffin, and 5 µm sections were cut and stained with H&E. In addition, frozen sections were cut from the eyes of 3 WT and 3 KO mice at 4 weeks of age and 12 months of age. The status of the cones was assessed by peanut agglutin (PNA; Alexa Fluor 488 conjugated PNA; Invitrogen Corp., Carlsbad, CA, USA) staining and co-stained with diamino-2-phenylindol (DAPI; Molecular Probes, Life Technologies, Carlsbad, CA, USA).

The retinas of 3 WT and 4 KO mice at 12 weeks of age were studied by immunohistochemistry. The mouse retinas were fixed, embedded in agarose, and cut into 50 µm thick sections by Linear Slicer PRO7 (Dosaka EM Co. Ltd., Kyoto, Japan). For immunostaining, we used anti-PKCalpha antibody (mouse monoclonal, P5704; Sigma-Aldrich, St. Louis, MO, USA), anti-S-opsin antibody (rabbit polyclonal, C1116; Santa Cruz, CA, USA), anti-M-opsin antibody (rabbit polyclonal, AB5405, Millipore, CA, USA), and anti-cone arrestin antibody (rabbit polyclonal, AB15282, Millipore, CA, USA). The antibody against mGluR6 was raised in guinea pigs with synthetic peptides (KKTSTMAAPPKSENSEDAK; 853-871, GenBank #NP_775548.2) as described in detail in Ref. 15. Sections were examined with an LSM900 confocal microscope (Carl Zeiss Microscopy, Jena, Germany).

Retinal Flat Mounts

For the retinal flat mount preparations, the mice were euthanized, and a slit was made in the lower part of the cornea to mark the orientation of the eye. The eyes were enucleated and fixed in 4% paraformaldehyde in phosphate-buffered saline (PBS) for 1 hour at room temperature. The cornea and lens were then removed, and after washing the eyecup 3 times with Tween 20 (0.02%) in PBS, they were blocked in 3% bovine serum albumin overnight at 4°C. They were then labeled with PNA in PBS overnight. To make the flat mounts, the entire retina was carefully dissected from the eyecup and radial cuts were made from the edges to the equator of the retinas while maintaining the orientation of the retina. The retinas were then washed 3 times with Tween 20 in PBS, then mounted flat on a glass slide and cover slipped. A fluorescence microscope (BZ-X800; Keyence, Osaka, Japan) was used to examine the retinal flat mounts, and images were taken at 20 times and 200 times magnification. Tissue sections were photographed using an optical sectioning system (structured illumination, SIM). At 200 times magnification, 8 z-axis positions separated by 1.2 µm were taken to generate clear images. The number of PNA-positive cells within a 720 µm × 540 µm area at 4 locations approximately 700 µm from the center of the optic disc was determined by an algorithm in the ImageJ software (http://imagej.nih.gov/ij/; provided in the public domain by the National Institutes of Health, Bethesda, MD, USA). After opening the images to be examined, the images were converted to a 16-bit greyscale. Once the areas of interest were highlighted, we created a binary version of the image. PNA-positive particles were then counted in each image using the automated counting feature of the ImageJ software. We calculated the cone photoreceptor density by determining the number of PNA-positive particles/mm^2 of retina. Then the means ± standard error of the mean of the cone photoreceptor densities from four different locations were calculated. The cone photoreceptor densities of 12 eyes of 12 WT mice and that of

Investigative Ophthalmology & Visual Science

6 eyes of 6 KO mice ranging from 4 to 24 weeks of age were compared.

RNA Sequencing

The total RNA from 4 eyes of 2 WT mice and 4 eyes of 2 KO mice at 4 weeks was isolated using the RNeasy Mini kit (Qiagen, Hilden, Germany). One sample was analyzed for each group. Library preparation was performed using 1 µg of the total RNA and TruSeq stranded mRNA Library Prep. The kit for Illumina (New England Biolabs, Ipswich, MA, USA) was used. The RNA-seq was done with an Illumina NovaSeq 6000 for 100 bp paired-end. Approximately 40 M reads were obtained for each sample. The reads were mapped against a mouse reference sequence, HISAT2 version 2.1.0, Bowtie2 version 2.3.5.1, a fast and sensitive alignment program for mapping next-generation sequencing reads. Sequencing reads were mapped to reference genome mouse (GRCm38/mm10, annotation RefSeq_2017_06_12). The expression level of each gene was quantified as fragments per kilobase of exon per million (FPKM) mapped fragments. The minimum requirement of total RNA to obtain commercially available RNA-Seq was more than RNA we could obtain from one retina sample. Thus, we performed RNA-Seq of four retina samples, which prevented us from statistical analysis.

Quantitative Real-Time PCR Analysis of Tissues from *Ctrp9*-KO Mice

The mice were anesthetized and the eyes were enucleated. The entire retina was carefully dissected from the eyecup. Both retinas from one mouse were combined. Total retinal RNA was extracted from 4 WT mice and 4 KO mice at 4 weeks using Sepasol-RNA 1 Super G (Nacalai Tesque, Inc., Kyoto, Japan). Then, cDNA was synthesized using PrimeScript 2 Reverse Transcriptase (Takara Bio, Shiga, Japan). Quantitative real-time PCR was performed using SYBR GreenER qPCR SuperMix Universal (Invitrogen, Carlsbad, CA, USA) and Thermal Cycler Dice Real-Time System single TP870 (Takara Bio) according to the manufacturer's instructions. Quantification was carried out by Thermal Cycler Dice Real-Time System Software version 3.00D (Takara Bio). Actin-b was used to normalize the amount of mRNA. The primer sequences are listed in Supplementary Table S1, and several sequences of these primers have been reported.[16,17]

Statistical Analyses

Data are presented as the means ± standard error of the means (SEM). Mann–Whitney *U* tests were used to determine the significance of differences in the degrees of gene expression in the retina. Repeated measures ANOVA was used to determine the significance of any differences in the ERG amplitudes. A P value of < 0.05 was considered statistically significant.

Results

Photopic B-Wave Amplitude Reduced in *Ctrp9*-KO Mice

Representative scotopic and photopic ERGs recorded from WT mice and *Ctrp9*-KO mice at 8 and 24 weeks of age are shown in Figure 1. The stimulus intensity-response curves

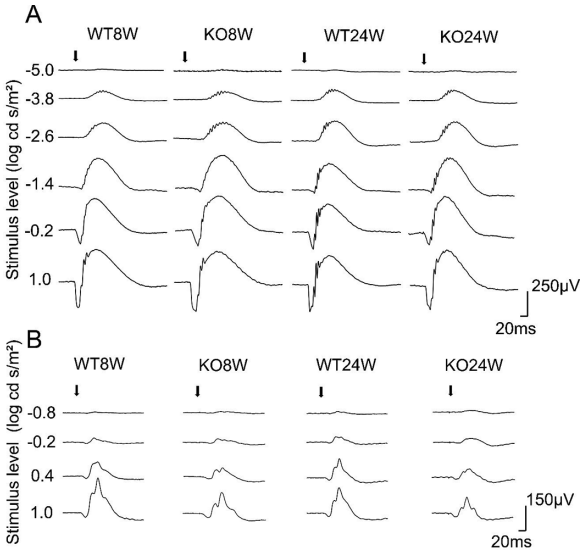

Figure 1. Scotopic (**A**) and photopic (**B**) ERGs of wild type (WT) mice and *Ctrp9*-KO mice elicited by different intensity stimuli are shown. The ERGs were recorded from 8-week-old (W) and 24-week-old WT and *Ctrp9*-KO mice. *Arrows* indicate the flash light stimuli. There are no obvious differences in the waveforms of the scotopic ERGs between the WT mice and KO mice **A**, but an attenuation of the photopic ERGs at 0.4 and 1.0 log cd s/m^2 in KO mice **B** can be seen at both ages.

of the WT mice and KO mice at 8 and 24 weeks of age are shown in Figure 2. The scotopic ERGs elicited by each stimulus level did not differ between the two types of mice. There were no significant differences in the scotopic a- and b-wave amplitudes between WT mice and KO mice at all stimulus levels at 8 and 24 weeks (Figs. 2A, 2B, 2D, 2E). On the other hand, the photopic ERGs were smaller at stimulus levels of 0.4 and 1.0 log cd s/m^2 in the KO mice than in the WT mice at 8 and 24 weeks (see Fig. 1B). The b-wave amplitudes in the KO mice were significantly smaller for 0.4 and 1.0 log cd s/m^2 at 24 weeks and at 1.0 log cd s/m^2 at 8 weeks (Figs. 2C, 2F, $P < 0.01$, repeated measures ANOVA). There were no significant differences in the amplitudes of the scotopic a- and b-waves and the photopic b-waves between 8 and 24 week old in KO mice. ERG findings in WT and KO mice at stimulus level of 1.0 log cd s/m^2 are shown in Supplementary Table S2. The implicit time of the photopic b-wave was 62.7 ± 1.6 ms (mean ± SEM) in the WT mice and 65.2 ± 1.0 ms in the KO mice, and there were no significant differences between WT mice and KO mice for 1.0 log cd s/m^2 at 8 weeks of age. On the other hand, the implicit time of the photopic b-wave were significantly delayed in the KO mice for stimulus level of 1.0 log cd s/m^2 at 24 weeks (WT = 50.4 ± 1.8 ms; KO = 60.0 ± 3.0 ms; $P < 0.01$: Mann–Whitney *U* test). There were no significant differences in the amplitudes of the oscillatory potentials between WT mice and KO mice at stimulus level of 1.0 log cd s/m^2 at 8 and 24 weeks of age. There were no significant differences in the photopic a-wave amplitudes between WT mice and KO mice at stimulus level of 1.0 log cd s/m^2 at 8 weeks. On the other hand, the photopic a-wave amplitudes were significantly smaller in the KO mice than that of the WT mice for 1.0 log cd s/m^2 at 24 weeks of age (WT = 22.3 ± 1.5 µV; KO = 15.5 ± 1.3 µV; $P < 0.01$: Mann–Whitney *U* test).

Investigative Ophthalmology & Visual Science

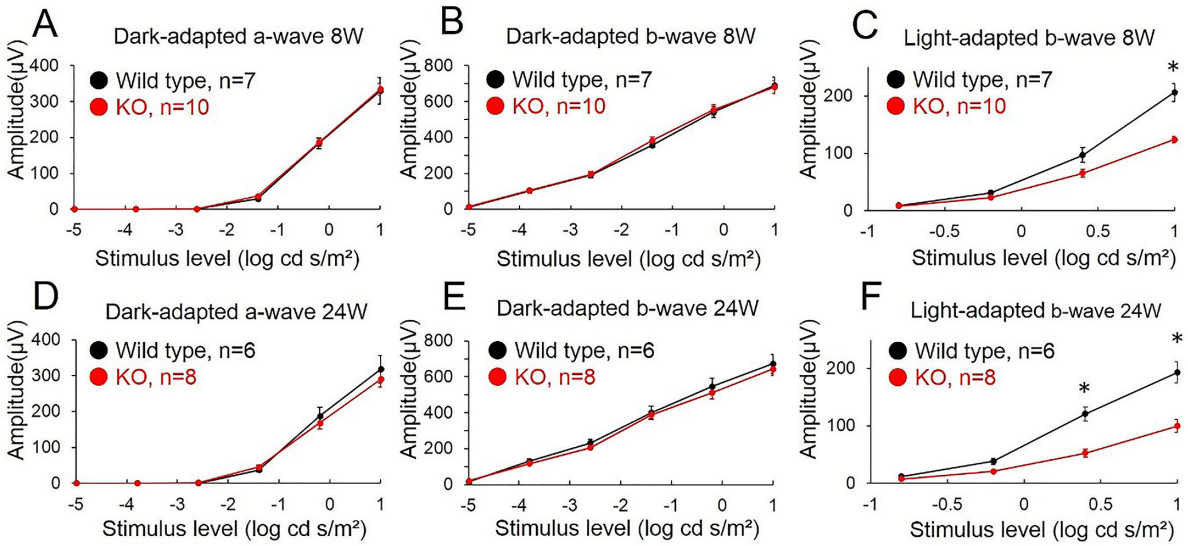

Figure 2. Intensity-response curves of scotopic and photopic ERG of WT and *Ctrp9*-KO mice. For the scotopic ERGs, the stimuli ranged from −5 to 1.0 log cd s/m^2 in 6 steps. The means and SEM of the scotopic a- and b-wave amplitudes are plotted. (**A**) The a-wave at 8 weeks; (**B**) b-wave at 8 weeks; (**D**) a-wave at 24 weeks; and (**E**) b-wave at 24 weeks. For the photopic ERGs, the means ± SEM amplitude of the b-waves elicited by stimuli that range from −0.8 to 1.0 log cd s/m^2 in 4 steps are plotted. (**C**) The b-wave at 8 weeks and (**F**) b-wave at 24 weeks. Seven WT mice and 10 KO mice at 8 weeks and 6 WT mice and 8 KO mice at 24 weeks were analyzed. There were no significant differences in the amplitudes of the scotopic a- and b-waves between WT mice and KO mice at both 8 and 24 weeks (**A, B, D, E**). But significant reductions of the amplitude of photopic b-waves at a stimulus level of 0.4 log cd s/m^2 in KO mice at 8 weeks **C** and at stimulus levels of 0.4 and 1.0 log cd s/m^2 in KO mice at 24 weeks **F** were found ($P < 0.01$, repeated measures ANOVA).

Reduction of Cone Photoreceptor Density in KO Mice

The results of the ERG studies indicated that the response of the cone pathway was reduced. To determine whether this was due to morphological alterations of the retinas, the retinas of 3 WT mice and 3 KO mice at 8 weeks and 24 weeks were stained with H&E. Because of the possibility of cone degeneration in the KO mice, we focused on the structure of the photoreceptor outer segments, inner segments, and the outer nuclear layers of the KO mice. We were not able to detect distinct differences between the two types of mice in the H&E sections at both ages (Fig. 3A). For further analysis on the status of the cone photoreceptors, we evaluated the retinal sections of 4-week-old and 12-month-old mice which were the oldest mice we were able to obtain for the analysis. The retinas were stained with PNA (Fig. 3B), and the signals of PNA appeared to be weaker in the KO mice at both ages. However, it was difficult to determine the differences in the staining from retinal sections. The PNA staining of the cone outer segments were visible in the 4-week-old and 12-month-old KO mice, and there appeared to be no significant differences between the 2 types of retinas. The findings suggested that the cone photoreceptors were still present at 12 months even in KO mice. Retinal sections from WT and KO mice were stained for cone opsin (M-opsin and S-opsin), cone arrestin, glutamatergic receptor (mGluR6), and PNA at 12 weeks (Fig. 3C). The results showed there were no apparent structural differences in the cones, retinal rod bipolar cells, and synaptic terminal of retinal bipolar cells between the two types of retinas.

We determined the density of the cone photoreceptors in the flat mounts stained with PNA (Fig. 4). The average cone photoreceptor density was evaluated at 4 locations approximately 700 µm from the optic disc for each mouse. The cone photoreceptor density was 6.4 ± 0.5 × 10^3 counts/mm^2 (mean ± SEM) in WT mice (n = 12) and 4.6 ± 0.5 × 10^3 counts/mm^2 in the KO mice ($P = 0.04$, $n = 6$, Mann–Whitney U test). This indicated that the cone photoreceptor density was reduced in KO mice by 28%.

Reduction of Expression of Cone-Related Gene in KO Mice

To evaluate the expression of the genes associated with the photoreceptor-related proteins, we performed genomewide RNA sequencing of 4-week-old WT and KO retinas. The mapped fragments were normalized for RNA length according to the FPKM mapped reads for each gene. This facilitated the comparisons of the transcript levels between the samples. The values of the FPKM of 29 photoreceptor genes are shown in Supplementary Table S3. Comparisons of the values of FPKM between KO mice and WT mice in the expression of the photoreceptor genes are shown in Figure 5. In the KO retina, some of the genes, such as *Opn1sw*, *Opn1mw*, *Ped6c*, *Cnga3*, and *Cngb3*, that are expressed only in cones were reduced to less than 60% of that in the WT retinas. On the other hand, the expression of the genes expressed in rods or both rods and cones showed no obvious reduction in KO mice. Genomewide RNA sequencing showed that *C1qtnf9*, the mRNA of *Ctrp9*, and other families *C1qtnf1*, *C1qtnf2*, *C1qtnf3*, *C1qtnf5*, *C1qtnf6*, *and C1qtnf7* were expressed at background level in both WT and KO mice (Supplementary Table S4). AdipoR1 and other newly reported receptors, calreticulin and N-cadherin,[18,19] were expressed in both types of the mice (see Supplementary Table S4).

Next, we performed quantitative real-time PCR analysis of nine photoreceptor-expressed genes (Fig. 6). The

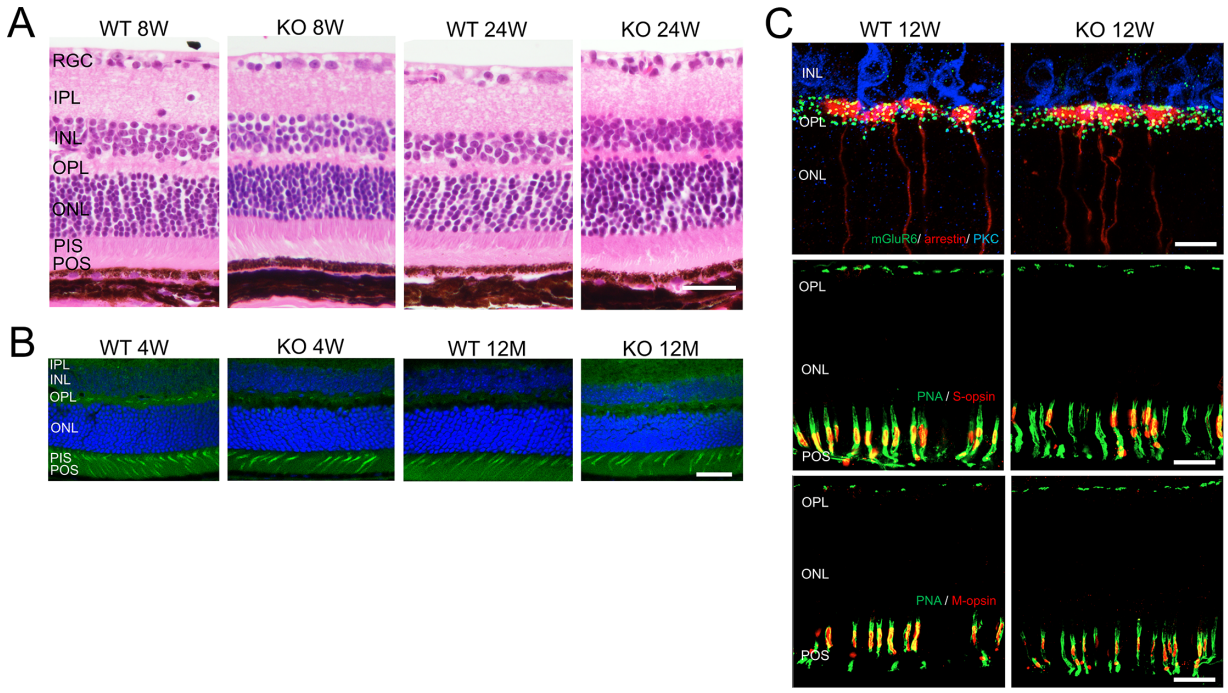

Figure 3. Retinal sections of WT mice and KO mice. (**A**) Representative hematoxylin and eosin stained retinal sections from WT mice and KO mice at 8 weeks and 24 weeks. The images were taken approximately 700 µm from the optic disc. No distinct histological differences were found between WT mice and KO mice at both ages. RGC, retinal ganglion cells; IPL, inner plexiform layer; INL, inner nuclear layer; OPL, outer plexiform layer; ONL, outer nuclear layer; PIS, photoreceptor inner segments; POS, photoreceptor outer segments. Scale bar: 50 µm. (**B**) Representative images of retinal sections stained with PNA (*green*) and DAPI (*blue*) from WT mice and KO mice at 4 weeks and 12 months. In each section, the PNA signals are clearly detected even in the retina of 12-month-old KO mouse. It is difficult to determine the differences of cone photoreceptor status by an examination of only the retinal sections. IPL, inner plexiform layer; INL, inner nuclear layer; OPL, outer plexiform layer; ONL, outer nuclear layer; PIS, photoreceptor inner segments; POS, photoreceptor outer segments. Scale bar: 50 µm. (**C**) Representative images of retinal sections stained with cone arrestin (*red at the top*), PKC (*blue at the top*), mGluR6 (*green at the top*), PNA (*green at the bottom and middle*), S-opsin (*red in the middle*), and M-opsin (*red at the bottom*) from WT mice and KO mice at 12 weeks. At 12 weeks, there was no significant structural differences in the cones and bipolar cells between WT and KO mice. INL, inner nuclear layer; OPL, outer plexiform layer; ONL, outer nuclear layer; POS, photoreceptor outer segments. Scale bar (*at the top*): 10 µm, Scale bar (*at the bottom and in the middle*): 20 µm.

expressions of *Opn1sw*, *Opn1mw*, *Gngt2*, and *Cnga3*, which are specifically expressed in cones, were significantly lower in KO mice than in WT mice. *Rxrg*, which is expressed only in cones, was lower in the KO mice but these differences were not reach significant. The amount of transcripts of the four other genes expressed in rods, *Rho*, *Gnat1*, and *Nrl*, or in both rods and cones (*Crx*) was not significantly different between the WT and KO mice.

Discussion

The results showed a reduction of the photopic ERGs in *Ctrp9*-KO mice which suggested that there was a decrease in the number of cones or that there was a decrease in the function due to damage of the individual cones. Abnormalities of the cone bipolar cells (e.g. fewer or dysfunctional cone bipolar cells), impaired synaptic transmission by the cones, or dysfunction of the light-adaptation mechanisms might also be the cause of the reduction of the cone ERGs. The results of counting the number of PNA-positive cells in the retinal flat mounts indicated that there was a reduction in cone photoreceptor number, which can explain the reduction in the ERG amplitudes, although we need to analyze the retinal cone bipolar cells and the synaptic terminal between cone and cone bipolar cells in more detail. Our findings indicated that there were no abnormalities in the rods because there were no abnormalities in retinal morphology and the scotopic ERGs.

We examined whether the decrease in the cone density was due to a progressive degeneration. In the KO mice, the rod and cone ERGs did not change between 8 and 24 weeks old mice, and PNA staining showed similar staining of the outer segments of the cones at both 4 weeks and 12 months. These results suggested that the absence of CTRP9 reduced the development of cone cells rather than causing a progressive degeneration of the cones although it is necessary to evaluate the number of cones during retinal development to make a more definitive conclusion.

The results of examining the expression of the gene transcripts in the RNA sequencing were similar to the comprehensive data for the high expression of *Rho*, *Gnat1*, and *Sag* in normal mouse retinas.[20] The gene transcripts belonging to most of the CTRP family, including CTRP9, were not expressed in either WT or KO retinas. In contrast, ADIPOR1 was expressed in the retina as reported.[20,21] In vivo studies showed that the expression of CTRP9 transcripts is relatively restricted to adipose tissues. The adiponectin and CTRP9 transcripts are rarely expressed in the eye.[4] In *Adipor1* KO mice, an impairment of DHA uptake causes a progressive degeneration of the photoreceptor cells from an early age,[11] which indicated that ADIPOR1 plays a crucial role in the retina. However, the absence of CTRP9 affected only the

Investigative Ophthalmology & Visual Science

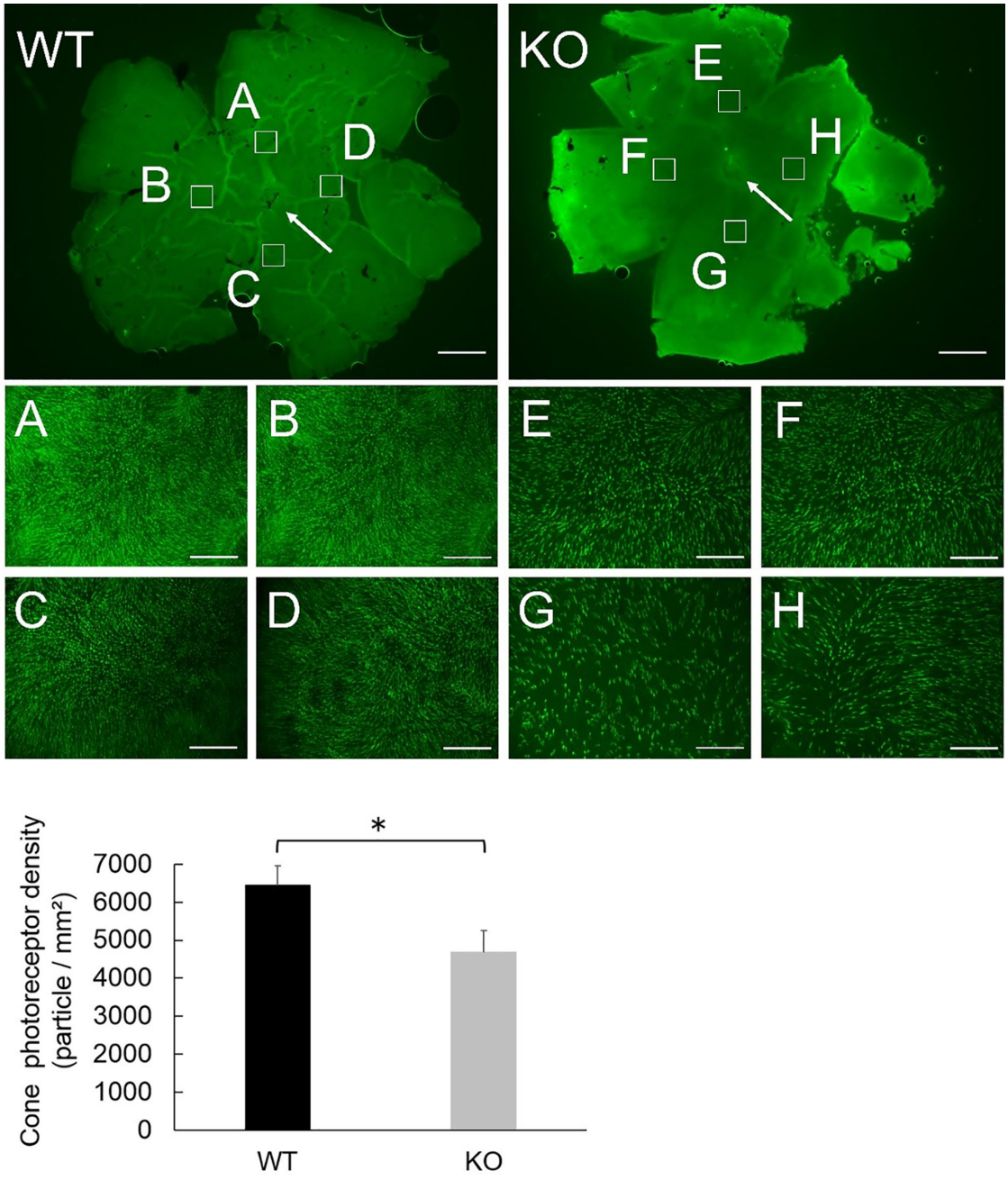

Figure 4. Representative images of retinal flat mounts from 4-week-old WT mice and KO mice. The retinal whole mounts were stained with PNA. The images of the entire flat mount at low magnification (20 times) from WT mouse and KO mouse are shown at the top (Scale bar: 700 µm). *Arrows* indicate the optic nerve disc. Four magnified images (times200) from the *white squares* of WT (**A–D**) and KO (**E–H**), which are located approximately 700 µm from the optic disc, are shown in the *middle*. The density of the PNA signals appear to be lower in the retina of KO mice than in WT mice (Scale bar: 70 µm). At the *bottom*, the average PNA positive particle density (particle/ mm^2; mean ± SEM), assumed to be cone photoreceptor density are shown (WT; $n = 12$ and KO; $n = 6$). The cone photoreceptor density was significantly lower in the KO mice ($P = 0.04$, Mann–Whitney U test).

number of cones and the phenotype was different from that of *Adipor1* KO mice. In *Adipor1*-null mice, a reduction of the retinal thickness and ERG responses was present at even 4 weeks of age.[11] On the other hand, *Ctrp9* KO mice showed less structural abnormalities with reduced amplitudes of the photopic ERGs. The reason why the phenotype of *Ctrp9*-KO was milder than that of *Adipor1* KO mice needs to be examined in the future, but ADIPOR1 may have multiple effects on the retina through other ligands or unknown pathways. In addition, there is the possibility that CTRP9 might affect the retina through other receptors, such as calreticulin and N-cadherin.[18,19]

The effects of CTRP9 on the retina have not been definitively determined. An overexpression of CTRP9 in mice can reduce the inflammation in diabetic retinopathy and disrupt the blood-retinal barrier.[22] A study on ARPE-19 cells reported that CTRP9 had antioxidative effects and prevented cell death that was caused by hyperglycemia.[12] The results

Investigative Ophthalmology & Visual Science

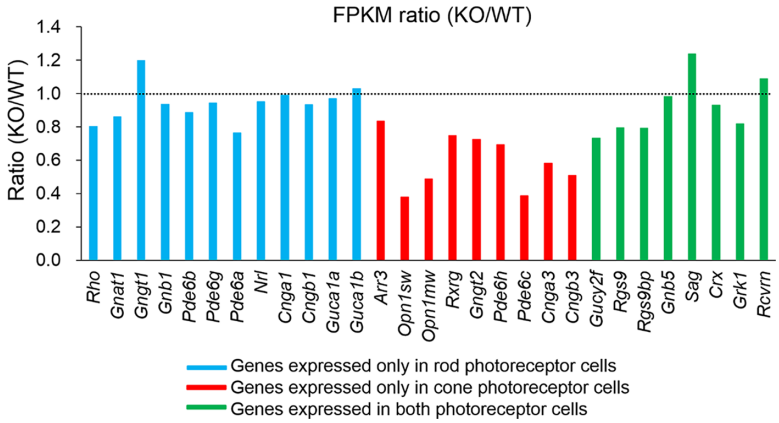

Figure 5. Comparison of photoreceptor-related genetic transcripts of WT mice to that of KO mice from genomewide RNA sequencing of the retinas. The ratios of WT to KO in the fragments per kilobase per million mapped (FPKM) reads are shown. Genes expressed only in rods, cones, and both are shown in *blue*, *red*, and *green*, respectively. In KO mice retina, some of the genes (*Opn1sw*, *Opn1mw*, *Ped6c*, *Cnga3*, and *Cngb3*) that are expressed only in cones were reduced to less than 60% of those in WT mice. On the other hand, the expressions of the genes expressed in rods or both the rods and cones were not reduced to that extent.

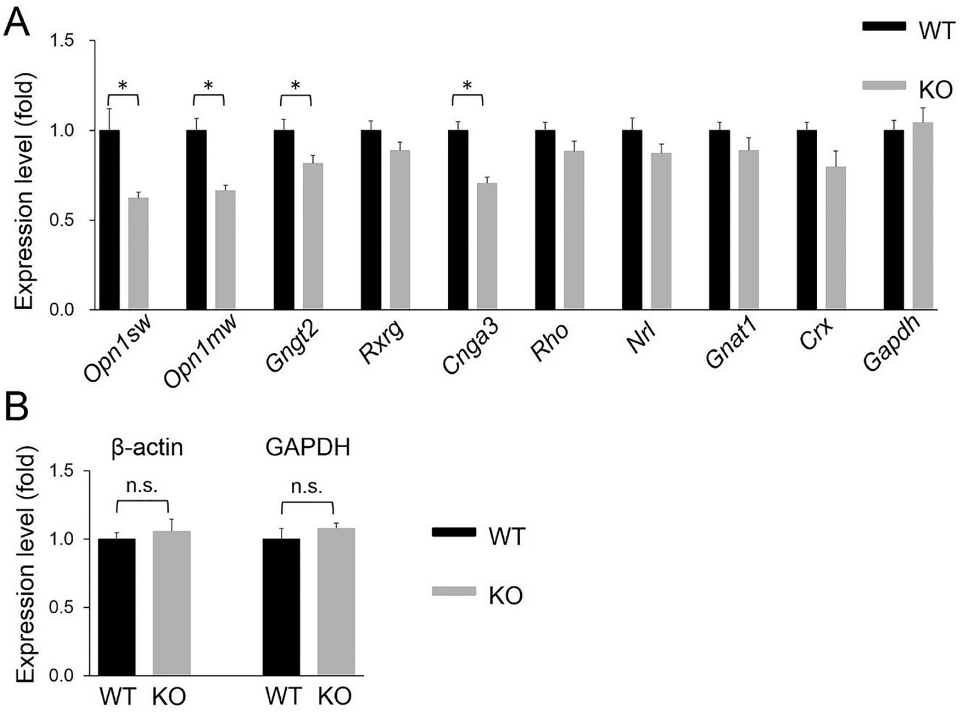

Figure 6. Comparisons between WT mice ($n = 4$) and KO mice ($n = 4$) in gene transcripts associated of photoreceptors evaluated by real-time RT-PCR. Relative expression levels (folds) of mRNA transcripts are shown for WT mice (*black*), KO mice (*gray*). (**A**) The expressions of *Opn1sw*, *Opn1mw*, *Cnga3*, *Gngt2*, and *Rxrg*, which are all expressed in cones, are lower in KO mice compared to WT mice. The expressions of *Opn1sw*, *Opn1mw*, *Gngt2*, and *Cnga3* were also significantly decreased. But the expressions of the other four genes which are expressed in rods (*Rho*, *Gnat1*, and *Nrl*) or all photoreceptors (*Crx*), are not significantly different between WT mice and KO mice. *$P < 0.05$ (Mann–Whitney U test). Values are the means ± SEMs. The expression level of indicated genes was normalized to that of the β-actin. (**B**) Real-time PCR analysis for β-actin and GAPDH mRNA are shown. The expression levels of indicated genes are normalized to the amount of total RNA. The mRNA expression of β-actin and GAPDH are not significantly different between the WT and KO mice, suggesting that these genes are suitable for internal controls (Mann–Whitney U test). n.s.: not significant. Values are the means ± SEMs.

of that study indicated that CTRP9 improved the glucose metabolism, anti-inflammation, and antioxidative and vasoprotective effects in the retina but there has been no mention on cone survival or development.

CTRP9 is known to be highly expressed in skeletal muscle, mammary glands, and in adipocytes.[3] Our data and previous studies indicate that adiponectin and CTRP9 transcript are rarely expressed in the retina,[4] although we did

not examine the expression profile of the RPE. Thus, the presence of CTRP9 in these tissues appears to regulate the retinal cone numbers to some degree.

The thyroid hormone, as a similar ectopic hormone, has been extensively studied for its crucial role as a modulator of cone opsin expression during photoreceptor differentiation. It has been reported that deletion of the thyroid hormone receptor $\beta 2$ (TR$\beta 2$), which is a ligand-activated transcription factor, caused a selective loss of the M cones and a concomitant increase in the S cones.[23] The thyroid hormone also regulates the expression of the cone opsin.[24–26] A similar function was suggested for the growth hormone.[27] These studies support the idea that the cone expression in mice is influenced by ectopically produced cytokines. However, unlike the thyroid hormones, CTRP9 does not appear to affect the differentiation of the S and M cones because the gene expression of the transcript was not different between *Opn1sw* (m-opsin) and *Opn1mw* (s-opsin). In addition, there was no marked structural difference in the S and M cones at the level of light microscopy between WT and KO retinas, although the gradient of S and M cones in the retina would be needed to make a definitive conclusion.

There are several limitations in our study. First, we only recorded ERGs up to 6 months, which might have overlooked a slow progressive retinal degeneration that occurs over a year. Second, we did not analyze the cone photoreceptors by electron microscopy, and thus have not examined the morphological changes of the fine structures of the photoreceptors. Third, the biggest problem was that the mechanism of the cone loss in KO mice was not determined. We tried to find clues for the mechanisms but failed. In the future, we will evaluate the expression of gene transcripts during cone development in the retina of KO mice. Fourth, immunohistochemical studies to confirm structural abnormalities of cone bipolar cells could not be performed because specific markers for bipolar cells were not available. In addition, statistical analysis to determine the fold change, false discovery rate (FDR), and pathway analyses were not possible because of the small number of samples in the RNA sequencing analyses.

In conclusion, our findings show that CRPT9, a ligand of AdipoR1, which is essential for the uptake of DHA in the retina, is released ectopically as an adipocytokine and acts to regulate the number of cones in the retina.

Acknowledgments

The authors thank Duco Hamasaki (Bascom Palmer Eye Institute) for the discussions and editing the final version of the manuscript.

Supported in part by the Japan Society for the Promotion of Science (JSPS) KAKENHI Grant Numbers 19K09928 to S.U., 19H03420 and 19K22426 to Y.O.

Disclosure: **D. Inooka**, None; **Y. Omori**, None; **N. Ouchi**, None; **K. Ohashi**, None; **Y. Kawakami**, None; **Y. Koyanagi**, None; **C. Koike**, None; **H. Terasaki**, None; **K.M. Nishiguchi**, None; **S. Ueno**, None

References

1. Ouchi N, Walsh K. Cardiovascular and metabolic regulation by the adiponectin/C1q/tumor necrosis factor-related protein family of proteins. *Circulation*. 2012;125:3066–3068.
2. Schäffler A, Buechler C. CTRP family: linking immunity to metabolism. *Trends Endocrinol Metab*. 2012;23:194–204.
3. Wu C, Orozco C, Boyer J, et al. BioGPS: an extensible and customizable portal for querying and organizing gene annotation resources. *Genome Biology*. 2009;10:R130.
4. Wong GW, Krawczyk SA, Kitidis-Mitrokostas C, et al. Identification and characterization of CTRP9, a novel secreted glycoprotein, from adipose tissue that reduces serum glucose in mice and forms heterotrimers with adiponectin. *FASEB J*. 2009;23:241–258.
5. Zheng Q, Yuan Y, Yi W, et al. C1q/TNF-related proteins, a family of novel adipokines, induce vascular relaxation through the adiponectin receptor-1/AMPK/eNOS/nitric oxide signaling pathway. *Arterioscler Thromb Vasc Biol*. 2011;31:2616–2623.
6. Kambara T, Shibata R, Ohashi K, et al. C1q/Tumor Necrosis Factor-Related Protein 9 Protects against Acute Myocardial Injury through an Adiponectin Receptor I-AMPK-Dependent Mechanism. *Mol Cell Biol*. 2015;35:2173–2185.
7. Yamauchi T, Kamon J, Ito Y, et al. Cloning of adiponectin receptors that mediate antidiabetic metabolic effects. *Nature*. 2003;423:762–769.
8. Xu M, Eblimit A, Wang J, et al. ADIPOR1 Is Mutated in Syndromic Retinitis Pigmentosa. *Hum Mutat*. 2016;37:246–249.
9. Zhang J, Wang C, Shen Y, et al. A mutation in *ADIPOR1* causes nonsyndromic autosomal dominant retinitis pigmentosa. *Hum Genet*. 2016;135:1375–1387.
10. Sluch VM, Banks A, Li H, et al. ADIPOR1 is essential for vision and its RPE expression is lost in the Mfrp(rd6) mouse. *Sci Rep*. 2018;8:14339.
11. Rice DS, Calandria JM, Gordon WC, et al. Adiponectin receptor 1 conserves docosahexaenoic acid and promotes photoreceptor cell survival. *Nat Commun*. 2015;6:6228.
12. Cheng Y, Qi Y, Liu S, et al. C1q/TNF-related Protein 9 Inhibits High Glucose-Induced Oxidative Stress and Apoptosis in Retinal Pigment Epithelial Cells Through the Activation of AMPK/Nrf2 Signaling Pathway. *Cell Transplantation*. 2020;29:963689720962052.
13. Valenzuela DM, Murphy AJ, Frendewey D, et al. High-throughput engineering of the mouse genome coupled with high-resolution expression analysis. *Nature Biotechnology*. 2003;21:652–659.
14. Ueno S, Kondo M, Miyata K, et al. Physiological function of S-cone system is not enhanced in rd7 mice. *Exp Eye Res*. 2005;81:751–758.
15. Koike C, Obara T, Uriu Y, et al. TRPM1 is a component of the retinal ON bipolar cell transduction channel in the mGluR6 cascade. *Proc. Natl. Acad. Sci. USA*. 2010;107:332–337.
16. Omori Y, Kubo S, Kon T, et al. Samd7 is a cell type-specific PRC1 component essential for establishing retinal rod photoreceptor identity. *Proc National Acad Sci USA*. 2017;114:E8264–E8273.
17. Omori Y, Kitamura T, Yoshida S, et al. Mef2d is essential for the maturation and integrity of retinal photoreceptor and bipolar cells. *Genes to Cells: Devoted to Molecular & Cellular Mechanisms*. 2015;20:408–426.
18. Zhao D, Feng P, Sun Y, et al. Cardiac-derived CTRP9 protects against myocardial ischemia/reperfusion injury via calreticulin-dependent inhibition of apoptosis. *Cell Death & Dis*. 2018;9:723.
19. Yan W, Guo Y, Tao L, et al. C1q/Tumor Necrosis Factor-Related Protein-9 Regulates the Fate of Implanted Mesenchymal Stem Cells and Mobilizes Their Protective Effects Against Ischemic Heart Injury via Multiple Novel Signaling Pathways. *Circulation*. 2017;136:2162–2177.
20. Gamsiz ED, Ouyang Q, Schmidt M, Nagpal S, Morrow EM. Genome-wide transcriptome analysis in murine neural

retina using high-throughput RNA sequencing. *Genomics*. 2012;99:44–51.

21. Osada H, Toda E, Homma K, et al. ADIPOR1 deficiency-induced suppression of retinal ELOVL2 and docosahexaenoic acid levels during photoreceptor degeneration and visual loss. *Cell Death & Dis*. 2021;12:458.
22. Li W, Ma N, Liu MX, et al. C1q/TNF-related protein-9 attenuates retinal inflammation and protects blood-retinal barrier in db/db mice. *Eur J Pharmacol*. 2019;853:289–298.
23. Ng L, Hurley JB, Dierks B, et al. A thyroid hormone receptor that is required for the development of green cone photoreceptors. *Nature Genetics*. 2001;27:94–98.
24. Glaschke A, Weiland J, Del Turco D, Steiner M, Peichl L, Glösmann M. Thyroid hormone controls cone opsin expression in the retina of adult rodents. *The Journal of Neuroscience: The Official Journal of the Society for Neuroscience*. 2011;31:4844–4851.
25. Glaschke A, Glösmann M, Peichl L. Developmental changes of cone opsin expression but not retinal morphology in the hypothyroid Pax8 knockout mouse. *Invest Ophthalmol Vis Sci*. 2010;51:1719–1727.
26. Mackin RD, Frey RA, Gutierrez C, et al. Endocrine regulation of multichromatic color vision. *Proc National Acad Sci USA*. 2019;116:16882–16891.
27. Novales Flamarique I, Sayed Ahmed A, Cheng CL, Molday RS, Devlin RH. Growth hormone regulates opsin expression in the retina of a salmonid fish. *J. Neuroendocrinol*. 2019;31:e12804.